Proceedings of the
46th IEEE Conference on Decision and Control
New Orleans, LA, USA, Dec. 12-14, 2007

Synchronized Control for Teleoperation with Different Configurations and Communication Delay

Hisanosuke Kawada, Kouei Yoshida and Toru Namerikawa

Abstract— **This paper deals with a control for teleoperation with different configurations and communication delays. We propose a synchronized control with individual gains and power scaling in the task space. In this method, the end-effector motion and force relationship between the master and slave robots can be specified freely in the task space and the control gains can be independently selected appropriately for the master and slave robots. The delay-independent asymptotic stability of the origin of the position and velocity errors is proven by using passivity of the systems and Lyapunov stability methods. The proposed control law achieves synchronization with power scaling. Several experimental results show the effectiveness of our proposed method.**

I. Introduction

Teleoperation is the extension of a person's sensing and manipulation capability to a remote location. A typical teleoperation system consists of a master robot and a slave robot and they are coupled via communication lines. The first goal is that the slave robot should track the positions of the master robot and the second goal is that the environmental force acting on the slave is accurately transmitted to the human operator. The most critical issues in the teleoperation are the time delay in communication line and the different configurations of the robots. The communication delay may destabilize the whole system. Then it is necessary to guarantee the stability for any communication delay [1]. Furthermore, the master and slave robots with different configurations act with different scales in several tasks involving teleoperation such as telesurgery and teleoperation of huge robotics for extra-vehicular activity. Then, the teleoperation with different configurations should be controlled on the end-effector motions in the task space and it is also necessary that the information of the motion and/or the force should be scaled between the master and slave robots. This scaling is called as the power scaling [8].

Stabilization for a teleoperation with the communication delay was achieved by the scattering transformation based on the idea of passivity [2] (This is equivalent to wave variable formulation [3]). Then, the additional structure with position control was proposed to solve the position drift [4], [5]. In [4] and [5], however, the stability of the system is dependent on the communication delay. In [6], it is shown that multi passive systems connected communication network with time delay can be synchronized by the coupling control law based on graph theory [7]. This approach is called as synchronized control. Moreover, the practical applicability of the result is demonstrated in the problem of teleoperation with any communication delay. The delay-independent asymptotic stability of the origin of the position and the velocity errors is guaranteed without the scattering transformation. In the above approaches [2], [4], [5], [6], however, the power scaling was not considered. In [8], [9], the power scaling for teleoperation with communication delay was achieved based on the scattering transformation approach. However, the position drift is caused by the traditional scattering approach without explicit position control. In [10], the teleoperation is decomposed in shape and locked systems and passive feedforward action is used to implement a scaled coordination between the master and slave robots. In this method, the communication delay was not treated. Furthermore, teleoperation with different configurations (including different scale) and communication delay have not been dealt with.

In this paper, we propose the synchronized control of teleoperation with different configurations and communication delays based on [6]. The master and slave robots are modeled as the task-space dynamical systems. Using the task-space feedback passivation, the new outputs which contain end-effector position and velocity information are utilized to guarantee the passivity. Then the master and slave robots are coupled together by using the synchronized control with power scaling and non-negligible communication delays. In addition, the gains of the synchronized control can be independently selected at the appropriate value for the master and slave robots. Therefore, the end-effector motion and force relationship between the master and slave robots can be specified freely in the task space. Using passivity of the systems and Lyapunov stability methods, the delay-independent asymptotic stability of the origin of the position and velocity errors is proven and the synchronization with power scaling is achieved. Finally several experimental results show the effectiveness of our proposed method.

II. Dynamics of Teleoperation

Assuming absence of friction and other disturbances, the master and slave robot dynamics with n-degree-of-freedom in the joint space are described as

$$\begin{cases} \boldsymbol{M_m}(\boldsymbol{q_m})\ddot{\boldsymbol{q}}_{\boldsymbol{m}} + \boldsymbol{C_m}(\boldsymbol{q_m}, \dot{\boldsymbol{q}}_{\boldsymbol{m}})\dot{\boldsymbol{q}}_{\boldsymbol{m}} + \boldsymbol{g_m}(\boldsymbol{q_m}) = \boldsymbol{\tau_m} + \boldsymbol{J_m^T F_{op}} \\ \boldsymbol{M_s}(\boldsymbol{q_s})\ddot{\boldsymbol{q}}_{\boldsymbol{s}} + \boldsymbol{C_s}(\boldsymbol{q_s}, \dot{\boldsymbol{q}}_{\boldsymbol{s}})\dot{\boldsymbol{q}}_{\boldsymbol{s}} + \boldsymbol{g_s}(\boldsymbol{q_s}) = \boldsymbol{\tau_s} - \boldsymbol{J_s^T F_{env}}, \end{cases} \tag{1}$$

where the subscript "m" and "s" denote the master and slave indexes respectively, $\boldsymbol{q}_m,\ \boldsymbol{q}_s \in \mathcal{R}^{n\times 1}$ are the joint

H. Kawada, K. Yoshida and T. Namerikawa are with Division of Electrical Engineering and Computer Science, Graduate School of Natural Science and Technology, Kanazawa University, Kakuma-machi, Kanazawa 920-1192 JAPAN. hisa@scl.ec.t.kanazawa-u.ac.jp, yoshida@scl.ec.t.kanazawa-u.ac.jp and toru@t.kanazawa-u.ac.jp

1-4244-1498-9/07/$25.00 ©2007 IEEE.

angle vectors, $\dot{\boldsymbol{q}}_{\boldsymbol{m}},\ \dot{\boldsymbol{q}}_{\boldsymbol{s}}, \in \mathcal{R}^{n\times 1}$ are the joint velocity vectors, $\ddot{\boldsymbol{q}}_{\boldsymbol{m}},\ \ddot{\boldsymbol{q}}_{\boldsymbol{s}}, \in \mathcal{R}^{n\times 1}$ are the joint acceleration vectors, $\boldsymbol{\tau_m},\ \boldsymbol{\tau_s} \in \mathcal{R}^{n\times 1}$ are the input torque vectors, $\boldsymbol{F_{op}} \in \mathcal{R}^{n\times 1}$ is the operational force vectors applied to the master robot by human operator, $\boldsymbol{F_{env}} \in \mathcal{R}^{n\times 1}$ is the environmental force vectors applied to the environment by the slave robot, $\boldsymbol{M_m},\ \boldsymbol{M_s} \in \mathcal{R}^{n\times n}$ are the symmetric and positive definite inertia matrices, $\boldsymbol{C_m}\dot{\boldsymbol{q}}_{\boldsymbol{m}},\ \boldsymbol{C_s}\dot{\boldsymbol{q}}_{\boldsymbol{s}} \in \mathcal{R}^{n\times 1}$ are the centripetal and Coriolis torque vectors and $\boldsymbol{g_m},\ \boldsymbol{g_s} \in \mathcal{R}^{n\times 1}$ are the gravitational torque vectors and $\boldsymbol{J_m},\ \boldsymbol{J_s} \in \mathcal{R}^{n\times n}$ are Jacobian matrices relating the end-effector velocity $\dot{\boldsymbol{x}}_{\boldsymbol{i}} \in \mathcal{R}^{n\times 1}$ to the joint velocity $\dot{\boldsymbol{q}}_{\boldsymbol{i}}$ as

$$\dot{\boldsymbol{x}}_{\boldsymbol{i}}(t) = \boldsymbol{J_i}(q_i)\dot{\boldsymbol{q}}_{\boldsymbol{i}}(t), \quad i = m, s. \tag{2}$$

For simplicity, we assume that

Assumption 1: The $\boldsymbol{J_m}(q_m)$ and $\boldsymbol{J_s}(q_s)$ are nonsingular matrices at all times in operation.

Above assumption is that we don't consider redundant robot and no kinematics singularities are encountered. Since the control at the task level, it is useful to rewrite the master and slave robot dynamics directly in the task space [12]. By further differentiation of (2) as

$$\ddot{\boldsymbol{x}}_{\boldsymbol{i}} = \boldsymbol{J_i}(q_i)\ddot{\boldsymbol{q}}_{\boldsymbol{i}} + \dot{\boldsymbol{J}}_{\boldsymbol{i}}(q_i)\dot{\boldsymbol{q}}_{\boldsymbol{i}}, \quad i = m, s, \tag{3}$$

where $\ddot{\boldsymbol{x}}_{\boldsymbol{m}}, \ddot{\boldsymbol{x}}_{\boldsymbol{s}} \in \mathcal{R}^{n\times 1}$ are the end-effector acceleration vectors and substitution (2) and (3) into (1), it is easy to see that the master and slave robots dynamics in the task space are described as

$$\begin{cases} \widetilde{\boldsymbol{M}}_{\boldsymbol{m}}(\boldsymbol{q_m})\ddot{\boldsymbol{x}}_{\boldsymbol{m}} + \widetilde{\boldsymbol{C}}_{\boldsymbol{m}}(\boldsymbol{q_m}, \dot{\boldsymbol{q}}_{\boldsymbol{m}})\dot{\boldsymbol{x}}_{\boldsymbol{m}} + \widetilde{\boldsymbol{g}}_{\boldsymbol{m}}(\boldsymbol{q_m}) = \boldsymbol{J}_{\boldsymbol{m}}^{-T}\boldsymbol{\tau_m} + \boldsymbol{F_{op}} \\ \widetilde{\boldsymbol{M}}_{\boldsymbol{s}}(\boldsymbol{q_s})\ddot{\boldsymbol{x}}_{\boldsymbol{s}} + \widetilde{\boldsymbol{C}}_{\boldsymbol{s}}(\boldsymbol{q_s}, \dot{\boldsymbol{q}}_{\boldsymbol{s}})\dot{\boldsymbol{x}}_{\boldsymbol{s}} + \widetilde{\boldsymbol{g}}_{\boldsymbol{s}}(\boldsymbol{q_s}) = \boldsymbol{J}_{\boldsymbol{s}}^{-T}\boldsymbol{\tau_s} - \boldsymbol{F_{env}} \end{cases}, \tag{4}$$

where

$$\widetilde{\boldsymbol{M}}_{\boldsymbol{i}} = \boldsymbol{J}_{\boldsymbol{i}}^{-T}\boldsymbol{M_i}\boldsymbol{J}_{\boldsymbol{i}}^{-1}, \quad \widetilde{\boldsymbol{C}}_{\boldsymbol{i}} = \boldsymbol{J}_{\boldsymbol{i}}^{-T}(\boldsymbol{C_i} - \boldsymbol{M_i}\boldsymbol{J}_{\boldsymbol{i}}^{-1}\dot{\boldsymbol{J}}_{\boldsymbol{i}})\boldsymbol{J}_{\boldsymbol{i}}^{-1},$$
$$\widetilde{\boldsymbol{g}}_{\boldsymbol{i}} = \boldsymbol{J}_{\boldsymbol{i}}^{-T}\boldsymbol{g_i} \quad i = m, s. \tag{5}$$

It is well known that the dynamics (4) have several fundamental properties as follows [12].

Property 1: The inertia matrices $\widetilde{\boldsymbol{M}}_{\boldsymbol{m}}(\boldsymbol{q_m})$, $\widetilde{\boldsymbol{M}}_{\boldsymbol{s}}(\boldsymbol{q_s})$ are symmetric and positive definite and there exist some positive constant m_{i1} and m_{i2} such that

$$0 < m_{i1}\boldsymbol{I} \le \widetilde{\boldsymbol{M}}_{\boldsymbol{i}}(\boldsymbol{q_i}) \le m_{i2}\boldsymbol{I} \quad i = m, s. \tag{6}$$

Property 2: Under an appropriate definition of the matrices $\widetilde{\boldsymbol{C_m}}(\boldsymbol{q_m}, \dot{\boldsymbol{q}}_{\boldsymbol{m}})$ and $\widetilde{\boldsymbol{C}}_{\boldsymbol{s}}(\boldsymbol{q_s}, \dot{\boldsymbol{q}}_{\boldsymbol{s}})$, the matrices $\boldsymbol{N_m}(\boldsymbol{q_m}, \dot{\boldsymbol{q}}_{\boldsymbol{m}}) = \dot{\widetilde{\boldsymbol{M}}}_{\boldsymbol{m}}(\boldsymbol{q_m}) - 2\widetilde{\boldsymbol{C}}_{\boldsymbol{m}}(\boldsymbol{q_m}, \dot{\boldsymbol{q}}_{\boldsymbol{m}})$ and $\boldsymbol{N_s}(\boldsymbol{q_s}, \dot{\boldsymbol{q}}_{\boldsymbol{s}}) = \dot{\widetilde{\boldsymbol{M}}}_{\boldsymbol{s}}(\boldsymbol{q_m}) - 2\widetilde{\boldsymbol{C}}_{\boldsymbol{s}}(\boldsymbol{q_m}, \dot{\boldsymbol{q}}_{\boldsymbol{m}})$ are skew symmetric such that

$$\boldsymbol{z}^T\boldsymbol{N_i}(\boldsymbol{q_i}, \dot{\boldsymbol{q}}_{\boldsymbol{i}})\boldsymbol{z} = 0, \quad i = m, s, \tag{7}$$

where $\boldsymbol{z} \in R^{n\times 1}$ is any vector.

Furthermore we assume for the stability analysis in later section as follows

Assumption 2: The communication delays between the master and slave robots are any asymmetric constant value as $T_m \ge 0$ and $T_s \ge 0$.

Assumption 3: The human operator and the environment can be modeled as passive systems, respectively.

Assumption 4: The operational and the environmental force $\boldsymbol{F_{op}}$ and $\boldsymbol{F_{env}}$ are bounded by functions of the master and slave robots signals respectively.

Assumption 5: All signals belong to $\mathcal{L}_{2e}$, the extended $\mathcal{L}_2$ space.

III. Control Objects

We would like to design $\boldsymbol{\tau_m}$ and $\boldsymbol{\tau_s}$ in (4) to achieve a task-space synchronization and static force reflection for the teleoperation with different configurations and communication delay. Let us define the position tracking errors of the end-effector with power scaling as

$$\begin{cases} \boldsymbol{e_m}(t) = \alpha^{-1}\boldsymbol{x_s}(t - T_s) - \boldsymbol{x_m}(t) \\ \boldsymbol{e_s}(t) = \alpha\boldsymbol{x_m}(t - T_m) - \boldsymbol{x_s}(t) \end{cases} \tag{8}$$

where $\alpha \in \mathcal{R}$ is a positive scalar and it expresses a motion scaling effect. $\boldsymbol{x_m}, \boldsymbol{x_s} \in \mathcal{R}^{n\times 1}$ are the end-effector position vectors. Then the control objects in this paper are: 1) the synchronization of teleoperation is achieved as

$$\boldsymbol{e_i}(t), \dot{\boldsymbol{e}}_{\boldsymbol{i}}(t) \to 0 \quad as \quad t \to \infty \qquad i = m, s \tag{9}$$

and 2) static force reflection is achieved with $\ddot{\boldsymbol{x}}_{\boldsymbol{i}}(t) = \dot{\boldsymbol{x}}_{\boldsymbol{i}}(t) = 0, \quad i = m, s$ as

$$\beta\boldsymbol{F_{op}} = \boldsymbol{F_{env}} \tag{10}$$

where $\beta \in \mathcal{R}$ is a positive scalar and it expresses a force scaling effect.

IV. Control Design

To achieve the synchronized teleoperation system, we design the master and slave robot controllers.

A. Feedback Passivation

the master and slave robot inputs are given as,

$$\begin{cases} \boldsymbol{\tau_m} = \boldsymbol{J}_{\boldsymbol{m}}^T\{-\widetilde{\boldsymbol{M}}_{\boldsymbol{m}}(q_m)\boldsymbol{\Lambda}\dot{\boldsymbol{x}}_{\boldsymbol{m}} - \widetilde{\boldsymbol{C}}_{\boldsymbol{m}}(q_m, \dot{q}_m)\boldsymbol{\Lambda}\boldsymbol{x_m} + \widetilde{\boldsymbol{g}}_{\boldsymbol{m}}(q_m) + \boldsymbol{F_m}\} \\ \boldsymbol{\tau_s} = \boldsymbol{J}_{\boldsymbol{s}}^T\{-\widetilde{\boldsymbol{M}}_{\boldsymbol{s}}(q_s)\boldsymbol{\Lambda}\dot{\boldsymbol{x}}_{\boldsymbol{s}} - \widetilde{\boldsymbol{C}}_{\boldsymbol{s}}(q_s, \dot{q}_s)\boldsymbol{\Lambda}\boldsymbol{x_s} + \widetilde{\boldsymbol{g}}_{\boldsymbol{s}}(q_s) + \boldsymbol{F_s}\} \end{cases} \tag{11}$$

where $\boldsymbol{F_m}$ and $\boldsymbol{F_s}$ are the additional inputs required for synchronized control in the next section and $\boldsymbol{\Lambda} = \mathrm{diag}(\lambda_1, \cdots, \lambda_n) \in \mathcal{R}^{n\times n}$ is a positive definite diagonal control gain matrix. Substituting (11) into (4), the master and slave robot dynamics are represented as

$$\begin{cases} \widetilde{\boldsymbol{M}}_{\boldsymbol{m}}(q_m)\dot{\boldsymbol{r}}_{\boldsymbol{m}} + \widetilde{\boldsymbol{C}}_{\boldsymbol{m}}(q_m, \dot{q}_m)\boldsymbol{r_m} = \boldsymbol{F_{op}} + \boldsymbol{F_m} \\ \widetilde{\boldsymbol{M}}_{\boldsymbol{s}}(q_s)\dot{\boldsymbol{r}}_{\boldsymbol{s}} + \widetilde{\boldsymbol{C}}_{\boldsymbol{s}}(q_s, \dot{q}_s)\boldsymbol{r_s} = -\boldsymbol{F_{env}} + \boldsymbol{F_s} \end{cases} \tag{12}$$

where the vector $\boldsymbol{r_m}$ and $\boldsymbol{r_s}$ are the new outputs of the master and slave robots and these are defined by linear combinations of the end-effector position and velocity vectors as

$$\begin{cases} \boldsymbol{r_m}(t) = \dot{\boldsymbol{x}}_{\boldsymbol{m}}(t) + \boldsymbol{\Lambda}\boldsymbol{x_m}(t) \\ \boldsymbol{r_s}(t) = \dot{\boldsymbol{x}}_{\boldsymbol{s}}(t) + \boldsymbol{\Lambda}\boldsymbol{x_s}(t). \end{cases} \tag{13}$$

Fig. 1 shows a block diagram of the master and slave robots with feedback passivation. Then we have the following lemma.

Lemma 1: Consider the systems described by (12) and define the inputs of the master and slave robot dynamics as $\acute{\boldsymbol{F}}_{\boldsymbol{m}} = \boldsymbol{F_m} + \boldsymbol{F_{op}}$ and $\acute{\boldsymbol{F}}_{\boldsymbol{s}} = \boldsymbol{F_s} - \boldsymbol{F_{env}}$ and the outputs as $\boldsymbol{r_m}$ and $\boldsymbol{r_s}$ respectively. Then, under *Assumption 1*, the

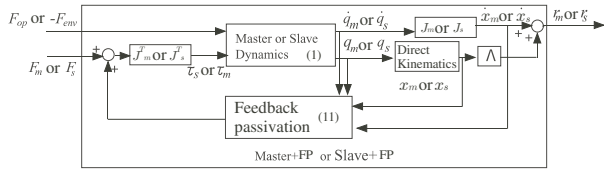

Fig. 1. the master and slave dynamics with nonlinear compensation

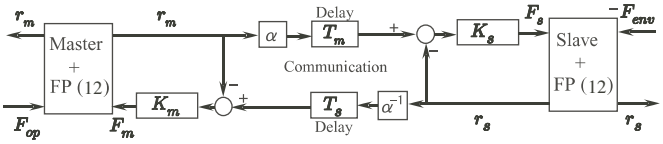

Fig. 2. The synchronized control architecture

systems with the above input and outputs are passive such that

$$\int_0^t \boldsymbol{r_i}^T(z)\dot{\boldsymbol{F}}_{\boldsymbol{i}}(z)dz \geq -\beta, \quad i = m, s. \tag{14}$$

Proof: This result follows easily by using following positive definite energy functions for the systems as

$$V_i(r_i(t)) = \frac{1}{2}\boldsymbol{r_i}^T(t)\widetilde{\boldsymbol{M_i}}(q_i)\boldsymbol{r_i}(t). \quad i = m, s. \tag{15}$$

■

Using feedback passivation as (11), the master and slave robot dynamics are passive with respect to the new outputs (13) which contain both the end-effector position and velocity information. Thus the teleoperation can be controlled in the passivity framework for the end-effector position and velocity signals by the new outputs.

B. Synchronized Control Law with Power Scaling

We propose the following synchronized control law considering different configurations and power scaling,

$$\begin{cases} \boldsymbol{F_m}(t) = \boldsymbol{K_m}(\alpha^{-1}\boldsymbol{r_s}(t - T_s) - \boldsymbol{r_m}(t)) \\ \boldsymbol{F_s}(t) = \boldsymbol{K_s}(\alpha\boldsymbol{r_m}(t - T_m) - \boldsymbol{r_s}(t)) \end{cases} \tag{16}$$

where $\boldsymbol{K_m}$ and $\boldsymbol{K_s}$ are defined as follows

$$\begin{cases} \boldsymbol{K_m} = k_m\boldsymbol{K} \\ \boldsymbol{K_s} = k_s\boldsymbol{K} \end{cases} \tag{17}$$

and $\boldsymbol{K} \in \mathcal{R}^{n\times n}$ is a positive definite diagonal control gain matrix and $k_m \in \mathcal{R}$ and $k_s \in \mathcal{R}$ are positive control gains for the master and slave robots respectively and $\alpha \in \mathcal{R}$ is a positive motion scaling factor. Compared with the conventional method in [6], where the gains of the master and slave side should be equal as $\boldsymbol{K_m} = \boldsymbol{K_s} = \boldsymbol{K}$ due to the stability analysis, the gains of proposed control law (16) can be independently selected at the appropriate value for the master and slave robots. In addition, the delayed feedback and feedforward signals are multiplied by a motion scaling factor. Fig. 2 shows a block diagram of the proposed teleoperation system. The "Master+FP" and "Slave+FP" show the master's and the slave's reduced dynamics in (12).

V. Stability Analysis

In this section we analyze the proposed synchronized control law with a power scaling and individual control gains previously and show that the control objectives are successfully fulfilled.

Theorem 1: Consider the system described by (12), (16) and (17). Then, under *Assumption 1-5*, the origin of the position tracking errors given by (8) $\boldsymbol{e_m}$,$\boldsymbol{e_s}$ and its derivatives $\dot{\boldsymbol{e}}_{\boldsymbol{m}}$, $\dot{\boldsymbol{e}}_{\boldsymbol{s}}$ are delay-independent asymptotically stable. Therefore the teleoperation is synchronized and power scaled.

Proof: Define a function for the system with respect to state vector $\boldsymbol{x}(t) = \left[\boldsymbol{r_m}^T, \boldsymbol{r_s}^T, \boldsymbol{e_m}^T, \boldsymbol{e_s}^T\right]^T$ as

$$\begin{aligned} V_{ms}(x) =& \alpha k_m^{-1}\boldsymbol{r_m}^T(t)\widetilde{\boldsymbol{M}}_{\boldsymbol{m}}(\boldsymbol{q_m})\boldsymbol{r_m}(t) + \alpha^{-1}k_s^{-1}\boldsymbol{r_s}^T(t)\widetilde{\boldsymbol{M}}_{\boldsymbol{s}}(\boldsymbol{q_s})\boldsymbol{r_s}(t) \\ &+ \alpha\boldsymbol{e_m}^T(t)\boldsymbol{\Lambda K e_m}(t) + \alpha^{-1}\boldsymbol{e_s}^T(t)\boldsymbol{\Lambda K e_s}(t) \\ &+ 2\alpha k_m^{-1}\int_0^t\{-\boldsymbol{F_{op}}^T(\zeta)\boldsymbol{r_m}(\zeta)\}d\zeta \\ &+ 2\alpha^{-1}k_s^{-1}\int_0^t\{\boldsymbol{F_{env}}^T(\zeta)\boldsymbol{r_s}(\zeta)\}d\zeta \\ &+ \int_{t-T_m}^t \alpha\boldsymbol{r_m}^T(\zeta)\boldsymbol{K r_m}(\zeta)d\zeta \\ &+ \int_{t-T_s}^t \alpha^{-1}\boldsymbol{r_s}^T(\zeta)\boldsymbol{K r_s}(\zeta)d\zeta \end{aligned} \tag{18}$$

First we prove that the function V_{ms} is positive definite. In (18), $\widetilde{\boldsymbol{M}}_{\boldsymbol{m}}$ and $\widetilde{\boldsymbol{M}}_{\boldsymbol{s}}$ are positive definite (by *Property 1*), α is positive, $\boldsymbol{K}$ and $\boldsymbol{\Lambda}$ are positive definite and the operator and the environment are passive (by *Assumption 3*) as

$$2\alpha^{-1}k_s^{-1}\int_0^t\left\{\boldsymbol{F_{env}}^T(\zeta)\boldsymbol{r_s}(\zeta)\right\}d\zeta \geq 0, \tag{19}$$

$$2\alpha k_m^{-1}\int_0^t\left\{-\boldsymbol{F_{op}}^T(\zeta)\boldsymbol{r_m}(\zeta)\right\}d\zeta \geq 0. \tag{20}$$

Thus the function V_{ms} is positive definite. The derivative of this function along trajectories of the system with the *Property 2* are given by

$$\begin{aligned} \dot{V}_{ms} =& 2\alpha k_m^{-1}\boldsymbol{r_m}^T\boldsymbol{F_m} + 2k_s^{-1}\alpha^{-1}\boldsymbol{r_s}^T\boldsymbol{F_s} \\ &+ 2\alpha\boldsymbol{e_m}^T\boldsymbol{\Lambda K}\dot{\boldsymbol{e}}_{\boldsymbol{m}} + 2\alpha^{-1}\boldsymbol{e_s}^T\boldsymbol{\Lambda K}\dot{\boldsymbol{e}}_{\boldsymbol{s}} \\ &+ \alpha\boldsymbol{r_m}^T\boldsymbol{K r_m} + \alpha^{-1}\boldsymbol{r_s}^T\boldsymbol{K r_s} \\ &- \alpha\boldsymbol{r_m}^T(t - T_m)\boldsymbol{K r_m}(t - T_m) \\ &- \alpha^{-1}\boldsymbol{r_s}^T(t - T_s)\boldsymbol{K r_s}(t - T_s) \end{aligned} \tag{21}$$

Substituting (16) into (21), we can get

$$\begin{aligned} \dot{V}_{ms} =& 2\alpha\boldsymbol{e_m}^T(t)\boldsymbol{\Lambda K}\dot{\boldsymbol{e}}_{\boldsymbol{m}}(t) + 2\alpha^{-1}\boldsymbol{e_s}^T(t)\boldsymbol{\Lambda K}\dot{\boldsymbol{e}}_{\boldsymbol{s}}(t) \\ &- \alpha\{\boldsymbol{r_m}(t) - \alpha^{-1}\boldsymbol{r_s}(t - T_s)\}^T\boldsymbol{K}\{\boldsymbol{r_m}(t) - \alpha^{-1}\boldsymbol{r_s}(t - T_s)\} \\ &- \alpha^{-1}\{\boldsymbol{r_s}(t) - \alpha\boldsymbol{r_m}(t - T_m)\}^T\boldsymbol{K}\{\boldsymbol{r_s}(t) - \alpha\boldsymbol{r_m}(t - T_m)\}. \end{aligned} \tag{22}$$

Substituting (13) and using (8), it can be rewritten as

$$\begin{aligned} \dot{V}_{ms} =& -\alpha\dot{\boldsymbol{e}}_{\boldsymbol{m}}^T(t)\boldsymbol{K}\dot{\boldsymbol{e}}_{\boldsymbol{m}}(t) - \alpha\boldsymbol{e_m}^T(t)\boldsymbol{\Lambda K\Lambda e_m}(t) \\ &- \alpha^{-1}\dot{\boldsymbol{e}}_{\boldsymbol{s}}^T(t)\boldsymbol{K}\dot{\boldsymbol{e}}_{\boldsymbol{s}}(t) - \alpha^{-1}\boldsymbol{e_s}^T(t)\boldsymbol{\Lambda K\Lambda e_s}(t) \end{aligned} \tag{23}$$

Thus the derivative of the Lyapunov function $\dot{V}_{ms}$ is negative semi-definite. To show the uniformly continuity of $\dot{V}_{ms}$, we

consider the derivative of $\ddot{V}_{ms}$ as follows,

$$\begin{aligned}\ddot{V}_{ms} = &-2\alpha\ddot{\boldsymbol{e}}_{\boldsymbol{m}}^T\boldsymbol{K}\dot{\boldsymbol{e}}_{\boldsymbol{m}} - 2\alpha\boldsymbol{e}_{\boldsymbol{m}}^T\boldsymbol{\Lambda}\boldsymbol{K}\boldsymbol{\Lambda}\dot{\boldsymbol{e}}_{\boldsymbol{m}} \\ &-2\alpha^{-1}\ddot{\boldsymbol{e}}_{\boldsymbol{s}}^T\boldsymbol{K}\dot{\boldsymbol{e}}_{\boldsymbol{s}} - 2\alpha^{-1}\dot{\boldsymbol{e}}_{\boldsymbol{s}}^T\boldsymbol{\Lambda}\boldsymbol{K}\boldsymbol{\Lambda}\boldsymbol{e}_{\boldsymbol{s}} \qquad (24)\end{aligned}$$

The $\dot{V}_{ms}$ is uniformly continuous, if the $\ddot{\boldsymbol{e}}_{\boldsymbol{m}}, \ddot{\boldsymbol{e}}_{\boldsymbol{s}}, \dot{\boldsymbol{e}}_{\boldsymbol{m}}, \dot{\boldsymbol{e}}_{\boldsymbol{s}}, \boldsymbol{e}_{\boldsymbol{m}}$ and $\boldsymbol{e}_{\boldsymbol{s}}$ are bounded. Since V_{ms} is lower-bounded by zero and $\dot{V}_{ms}$ is negative semi-definite, we can conclude that the signals $\boldsymbol{r}_{\boldsymbol{m}}, \boldsymbol{r}_{\boldsymbol{s}}, \boldsymbol{e}_{\boldsymbol{m}}$ and $\boldsymbol{e}_{\boldsymbol{s}}$ are bounded. Note that Laplace transform of (13) yields strictly proper, exponentially stable, transfer functions between $\boldsymbol{r}_{\boldsymbol{m}}, \boldsymbol{r}_{\boldsymbol{s}}$ and $\boldsymbol{x}_{\boldsymbol{m}}, \boldsymbol{x}_{\boldsymbol{s}}$ are given as,

$$\boldsymbol{X}_{\boldsymbol{i}}(\mathbf{s}) = \mathrm{diag}\Big(\frac{1}{\mathbf{s}+\lambda_1}, \cdots, \frac{1}{\mathbf{s}+\lambda_n}\Big)\boldsymbol{R}_{\boldsymbol{i}}(\mathbf{s}) \quad i = m, s \quad (25)$$

where "$\mathbf{s}$" is the Laplace variable, the $\boldsymbol{R}_{\boldsymbol{i}}(\mathbf{s})$ and $\boldsymbol{X}_{\boldsymbol{i}}(\mathbf{s})$ are the Laplace transform of the $\boldsymbol{r}_{\boldsymbol{i}}$ and $\boldsymbol{x}_{\boldsymbol{i}}$ respectively. Since $\boldsymbol{r}_{\boldsymbol{m}}, \boldsymbol{r}_{\boldsymbol{s}} \in \mathcal{L}_\infty$ and (25), the outputs of the system (25) will have the property $\dot{\boldsymbol{x}}_{\boldsymbol{m}}, \dot{\boldsymbol{x}}_{\boldsymbol{s}}, \boldsymbol{x}_{\boldsymbol{m}}, \boldsymbol{x}_{\boldsymbol{s}} \in \mathcal{L}_\infty$ [12] and $\dot{\boldsymbol{e}}_{\boldsymbol{m}}, \dot{\boldsymbol{e}}_{\boldsymbol{s}} \in \mathcal{L}_\infty$. From *Assumption 4*, the operational and the environmental force are bounded by the function of the $\boldsymbol{r}_{\boldsymbol{m}}, \boldsymbol{r}_{\boldsymbol{s}}$ as $\boldsymbol{F}_{\boldsymbol{op}}, \boldsymbol{F}_{\boldsymbol{env}} \in \mathcal{L}_\infty$. From (16), It is easy to see that $\boldsymbol{F}_{\boldsymbol{m}}, \boldsymbol{F}_{\boldsymbol{s}} \in \mathcal{L}_\infty$. Then we can get that $\boldsymbol{\tau}_{\boldsymbol{m}}, \boldsymbol{\tau}_{\boldsymbol{s}} \in \mathcal{L}_\infty$. From (4), the master and slave robot accelerations are bounded as $\ddot{\boldsymbol{x}}_{\boldsymbol{m}}, \ddot{\boldsymbol{x}}_{\boldsymbol{s}} \in \mathcal{L}_\infty$ which gives us that the signal $\ddot{\boldsymbol{e}}_{\boldsymbol{m}}$ and $\ddot{\boldsymbol{e}}_{\boldsymbol{s}}$ are bounded. Therefore $\ddot{V}_{ms}$ is bounded and $\dot{V}_{ms}$ is uniformly continuous. Applying Barbalat's Lemma [13] we can see that $\dot{V}_{ms}(x) \to 0$ as $t \to \infty$. The origin of the position tracking errors given by (8) $\boldsymbol{e}_{\boldsymbol{m}}$, $\boldsymbol{e}_{\boldsymbol{s}}$ and its derivatives $\dot{\boldsymbol{e}}_{\boldsymbol{m}}$, $\dot{\boldsymbol{e}}_{\boldsymbol{s}}$ are the delay-independent asymptotically stable. Therefore the teleoperation is synchronized and power scaled. ■

In the steady state, we can show that the contact force is transmitted to the master side.

Proposition 1: Consider the system described by (12), (16) and (17). Then, under the *Assumption 1-5* and the steady state as follows

$$\ddot{\boldsymbol{x}}_{\boldsymbol{i}}(t) = \dot{\boldsymbol{x}}_{\boldsymbol{i}}(t) = 0, \boldsymbol{x}_{\boldsymbol{i}}(t) = constant, \quad i = m, s, \qquad (26)$$

we obtain that the scaled contact force is accurately transmitted to the master robot side as follows

$$\beta\boldsymbol{F}_{\boldsymbol{op}} = k_s\boldsymbol{K}\boldsymbol{\Lambda}(\alpha\boldsymbol{x}_{\boldsymbol{m}} - \boldsymbol{x}_{\boldsymbol{s}}) = \boldsymbol{F}_{\boldsymbol{env}} \qquad (27)$$

where $\beta(=\alpha\frac{k_s}{k_m}) \in \mathcal{R}$ is a positive force scaling factor.

Proof: In the steady state (26), the master and slave dynamics (12) are reduced to

$$\begin{cases}\boldsymbol{F}_{\boldsymbol{op}} = -\boldsymbol{F}_{\boldsymbol{m}} = -k_m\boldsymbol{K}\boldsymbol{\Lambda}(\alpha^{-1}\boldsymbol{x}_{\boldsymbol{s}} - \boldsymbol{x}_{\boldsymbol{m}}) \\ \boldsymbol{F}_{\boldsymbol{env}} = \boldsymbol{F}_{\boldsymbol{s}} = k_s\boldsymbol{K}\boldsymbol{\Lambda}(\alpha\boldsymbol{x}_{\boldsymbol{m}} - \boldsymbol{x}_{\boldsymbol{s}})\end{cases} \qquad (28)$$

The above equations give

$$\alpha\frac{k_s}{k_m}\boldsymbol{F}_{\boldsymbol{op}} = k_s\boldsymbol{K}\boldsymbol{\Lambda}(\alpha\boldsymbol{x}_{\boldsymbol{m}} - \boldsymbol{x}_{\boldsymbol{s}}) = \boldsymbol{F}_{\boldsymbol{env}}. \qquad (29)$$

Therefore the scaled contact force is accurately transmitted to the master robot side. ■

Remark 1: From *Theorem 1* and *Proposition 1*, we can conclude the following properties

$\alpha > 1$: The motion of the slave is scaled up
$\alpha < 1$: The motion of the slave is scaled down
$\alpha = 1$: The slave is operated in a same scale motion
(β affects similarly the force of the slave)

The asymptotic stability is guaranteed when the scaling factors and controller gains are finite. Hence the proposed method can independently specify the scale of the motion and the force relationship between the master and slave robots by using α and β. The main advantages of the proposed control strategy are to scale with different factor of the signals of the motion and the force exchanged between the master and slave side and to guarantee the convergence of the position errors. Note that the controller gains k_m and k_s should be selected in the appropriate range. The smaller k_m and k_s may deteriorate the tracking performance and the larger ones may exceeds the physical constraints of the control inputs. Therefore, the force scaling factor should be selected considering $\beta = \alpha\frac{k_s}{k_m}$ under the restriction on the magnitudes of k_m and k_s.

VI. Evaluation by Control Experiments

In this section, we verify the efficacy of the proposed teleoperation methodology. The experiments were carried out on a couple of different configuration robots as shown in Figs. 3, 4 and 5. The master robot is planar serial-link arm with 2DOF and the slave robot is planar parallel-link arm with 2DOF. The inertia matrices, Coriolis matrices and Jacobian matrices of the master and slave robots are identified as follows

Master:

$$\boldsymbol{M}_{\boldsymbol{m}} = \begin{bmatrix}\theta_{m1} & \theta_{m2}\cos(q_{m1}-q_{m2}) \\ \theta_{m2}\cos(q_{m1}-q_{m2}) & \theta_{m3}\end{bmatrix},$$

$$\boldsymbol{C}_{\boldsymbol{m}} = \begin{bmatrix}0 & \theta_{m2}\dot{q}_{m2}\sin(q_{m1}-q_{m2}) \\ -\theta_{m2}\dot{q}_{m1}\sin(q_{m1}-q_{m2}) & 0\end{bmatrix}, \boldsymbol{g}_{\boldsymbol{m}} = 0,$$

$$\boldsymbol{J}_{\boldsymbol{m}} = \begin{bmatrix}-l_{m1}\sin(q_{m1}) & l_{m2}\sin(q_{m2}) \\ l_{m1}\cos(q_{m1}) & -l_{m2}\cos(q_{m2})\end{bmatrix}$$

$$\theta_{m1} = 0.00149[\mathrm{kgm}^2],\ \theta_{m2} = -0.000764[\mathrm{kgm}^2],\ \theta_{m3} = 0.000686[\mathrm{kgm}^2]$$

Slave:

$$\boldsymbol{M}_{\boldsymbol{s}} = \begin{bmatrix}\theta_{s1}+2\theta_{s3}\cos(q_{s2}) & \theta_{s2}+\theta_{s3}\cos(q_{s2}) \\ \theta_{s2}+\theta_{s3}\cos(q_{s2}) & \theta_{s2}\end{bmatrix},$$

$$\boldsymbol{C}_{\boldsymbol{s}} = \begin{bmatrix}-\theta_{s3}\sin(q_{s2})\dot{q}_{s2} & -\theta_{s3}\sin(q_{s2})(\dot{q}_{s1}+\dot{q}_{s2}) \\ \theta_{s3}\sin(q_{s2})\dot{q}_{s1} & 0\end{bmatrix}, \quad \boldsymbol{g}_{\boldsymbol{s}} = 0$$

$$\boldsymbol{J}_{\boldsymbol{s}} = \begin{bmatrix}-l_{s1}\sin(q_{s1}) - l_{s2}\sin(q_{s1}+q_{s2}) & -l_{s2}\sin(q_{s1}+q_{s2}) \\ l_{s1}\cos(q_{s1}) + l_{s2}\cos(q_{s1}+q_{s2}) & l_{s2}\cos(q_{s1}+q_{s2})\end{bmatrix},$$

$$\theta_{s1} = 0.366[\mathrm{kgm}^2],\ \theta_{s2} = 0.0291[\mathrm{kgm}^2],\ \theta_{s3} = 0.0227[\mathrm{kgm}^2].$$

Here the slave robot is larger than the master robot. Then we should scale up the motion from the master robot to

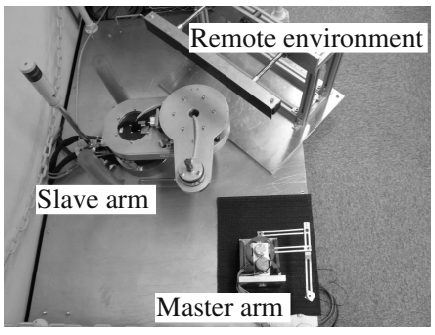

Fig. 3. Experiment setup

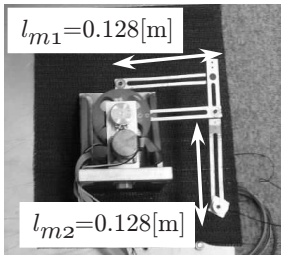

Fig. 4. Master arm

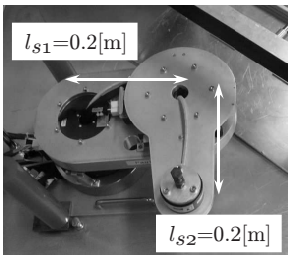

Fig. 5. Slave arm

the slave robot. We also measure the operational and the environmental force (i.e. $\boldsymbol{F_{env}}, \boldsymbol{F_{op}}$ in (4)) using the force sensors. We use a real-time calculating machine (dSPACE Inc.) and 1 [ms] sampling rate is obtained. The control programs are written in MATLAB and SIMULINK, and implemented using the Real-Time Workshop and dSPACE Software which includes Control Desk, Real-Time Interface and so on. We use the environment of an aluminum wall covered by a rubber as shown in Fig. 3.

The controller parameters $\boldsymbol{K}$, $\boldsymbol{\Lambda}$, k_m and k_s are selected as follows

$$\boldsymbol{\Lambda} = \begin{bmatrix} 5 & 0 \\ 0 & 5 \end{bmatrix}, \ \boldsymbol{K} = \begin{bmatrix} 5 & 0 \\ 0 & 5 \end{bmatrix}, \ \ k_m = 1, \ \ k_s = 6. \tag{30}$$

The scaling factor is selected considering the ratio of the length of the link ($l_{s1}/l_{m1} = 1.5625 \approx 1.5$) as $\alpha = 1.5$. Hence we expected that the motion of the slave robot is 1.5 times and the force of the slave robot is also $\beta = \alpha\frac{k_s}{k_m} = 9$ times as much as those of the master robot. All experiments have been done with an artificial constant communication delays of $T = T_m = T_s = 0.5$ [s]. Two kinds of experimental conditions are given as follows.

Case 1: The slave moves without any contact.

Case 2: The slave moves in contact with the environment.

In Case 1, we show the experimental comparison between the equivalent gains as $k_m = k_s = 1$ and the individual gain as (30). Figs. 6 - 9 show the results in Case 1. Fig. 6 shows time responses of the end-effector's X-positions in case of the equivalent gains as $k_m = k_s = 1$ and Fig. 8 shows time responses of the end-effector's X-positions in case of the individual gain as (30). From Figs. 6 (a) and 8 (a), the responses of the slave robot are almost α times as much as those of the master robot. Figs. 6 (b) and 8 (b) are modification of the above experimental data for comparison where the master robot responses are multiplied by α and shifted to 0.5[s] to cancel the communication delay. In Fig. 6 (b), there are the steady state errors due to physical coulomb friction and/or some disturbance of the robots. If gain $\boldsymbol{K}$ is larger, the errors are expected to become smaller. However, it is not possible to choose the larger gains, because the control gains are equivalent as $k_m = k_s = 1$ and the input torque command for the master robot are behind to its physical maximum torque (the physical maximum torque of the master are about 0.3 [Nm]) as shown in Fig. 7. On the other hand, in Fig. 8 (b), the positions of the slave robot accurately track those of the master robot and the synchronization with power scaling between the master and slave robots is achieved. Because the controller gains for the master and slave robots can be independently selected appropriately as (30).

Figs. 10-12 show the results in Case 2. As shown in Figs. 10 and 11, when the slave robot is pushing the environment (5-35 [s]), the contact force is faithfully reflected to the operator. The operator can perceive the environment through the force reflection. The environmental force responses are roughly β times as much as operational force responses. Fig. 12 is modification of the above experimental data for comparison where the position of master robot responses are multiplied by α, the force of master robot responses are multiplied by β and shifted to the right. From Fig. 12, the environmental forces on contact are accurately transmitted to the operator.

VII. Conclusions

In this paper, we proposed the task-space synchronized control for teleoperation with different configurations and communication delays. In this method, the motion and force relationship between the master and slave robots could be specified freely in the task space. The delay-independent asymptotic stability of the origin of the position and velocity errors was proven by using passivity of the systems and Lyapunov stability methods. The synchronization with power scaling and non-negligible communication delays was achieved. Finally several experimental results showed the effectiveness of our proposed method.

References

[1] P. F. Hokayem and M. W. Spong, "Bilateral teleoperation: An historical survey" *Automatica*, Vol. 42, No. 12, pp. 2035-2057, 2006.

[2] R. J. Anderson and M. W. Spong, "Bilateral Control of Teleoperators with Time Delay," *IEEE Trans. on Automatic Control*, Vol.34, No.5, pp. 494-501, 1989.

[3] G. Niemeyer and J. -J. E. Slotine, "Telemanipulation with Time Delays," *The Int. J. of Robotics Research*, Vol. 23, No.9, pp. 873-890, 2004.

[4] N. Chopra, M. W. Spong, R. Ortega and N. E. Barabanov, "On Tracking Performance in Bilateral Teleoperation," *IEEE Trans. on Robotic*s, Vol. 22, No. 4, pp. 861-866, 2006.

[5] T. Namerikawa and H. Kawada, "Symmetric Impedance Matched Teleoperation with Position Tracking," *In proc. of the 45th IEEE Conference on Decision and Control*, pp. 4496-4501, 2006.

[6] N. Chopra and M. W. Spong, "On Synchronization of Networked Passive Systems with Time Delays and Application to Bilateral Teleoperation," *In proc. of the SICE Annual Conference 2005*, pp. 3424-3429, 2005.

[7] R. Olfati-Saber and R. M. Murray, "Consensus Problems in Networks of Agents With Switching Topology and Time-Delays", *IEEE Trans. on Automatic Control*, Vol. 49, No. 9, pp. 1520-1533, 2004.

[8] K. Kosuge, T. Itoh and T. Fukuda, "Scaled telemanipulation with communication time delay," *In proc of the IEEE International Conference on Robotics and Automation*, pp. 2019-2024, 1996.

[9] C. Secchi, S. Straimgioli, C. Fantuzzi, "Power scaling in port-Hamiltonian based telemanipulation," *In proc. of the IEEE/RSJ International Conference on Intelligent Robots and Systems*, pp. 1850-1855, 2005.

[10] D. Lee and P. Y. Li, "Passive Bilateral Control and Tool Dynamics Rendering for Nonlinear Mechanical Teleoperators," *IEEE Trans on Robotics*, Vol. 21, No. 5, pp.936-950, 2005.

[11] H. Kawada and T. Namerikawa, "Passivity-based Synchronized Control of Teleoperation with Power Scaling," *In proc. of the SICE-ICASE International Joint Conference 2006*, pp. 1838-1843, 2006.

[12] C. C. de Wit, B. Siciliano and G. Bastin (Eds), *Theory of Robot Control*, Springer, 1996.

[13] H. K. Khalil, *Nonlinear systems*, Prentice-Hall, 1996.

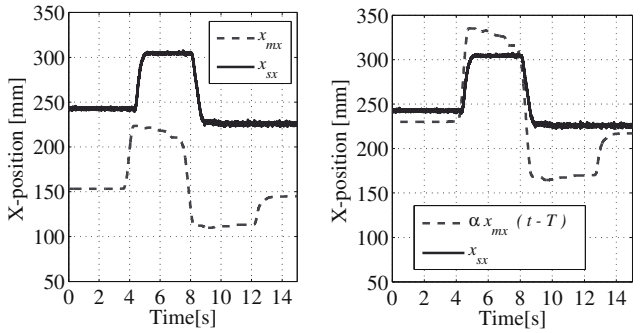

(a) Time response (b) Scaled and shifted data

Fig. 6. Position data in Case 1 (equivalent gain as $k_m = k_s = 1$)

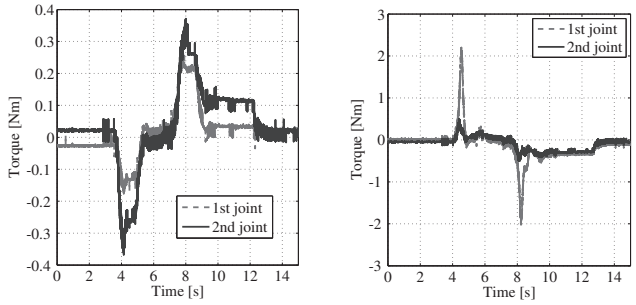

(a) Master robot (b) Slave robot

Fig. 7. Input torque command in Case 1(equivalent gain as $k_m = k_s = 1$)

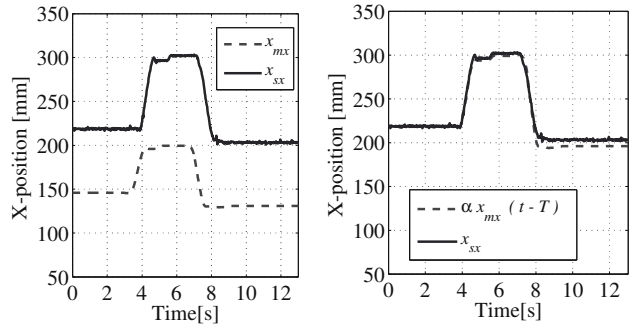

(a) Time response (b) Scaled and shifted data

Fig. 8. Position data in Case 1 (individual gain as (30))

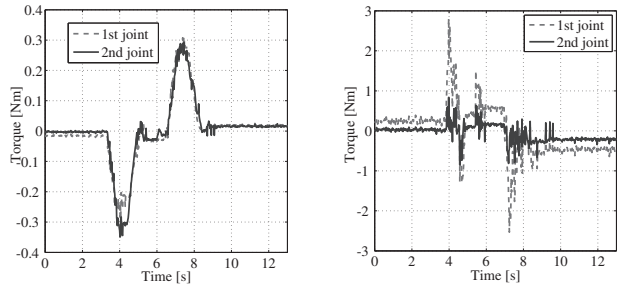

(a) Master robot (a) Slave robot

Fig. 9. Input torque command in Case 1 (individual gain as (30))

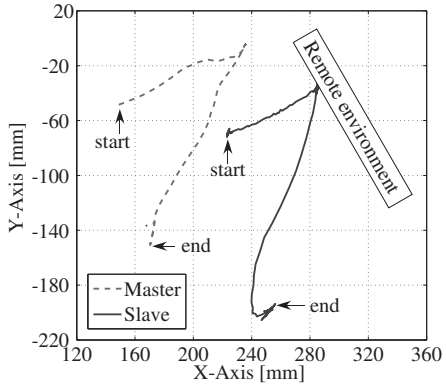

Fig. 10. Trajectories in Case 2 (proposed method)

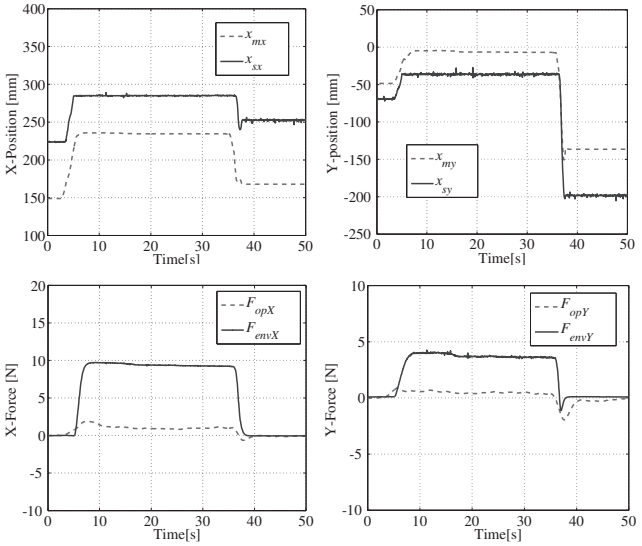

Fig. 11. Time responses in Case 2

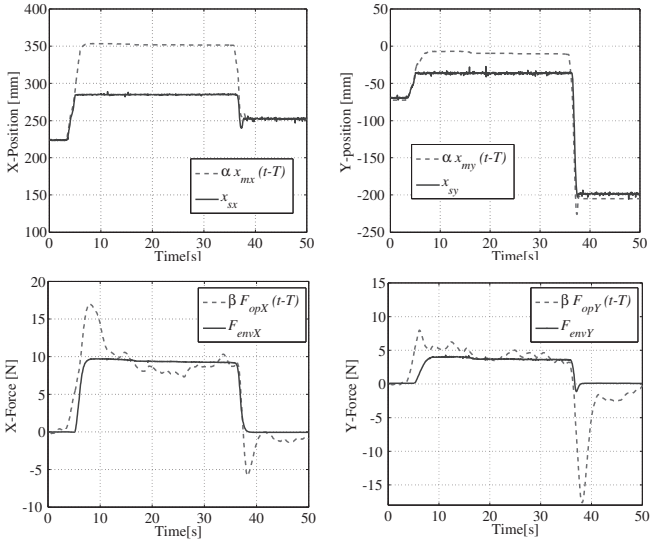

Fig. 12. Shifted and scaled response results of Fig. 11